Available online at www.sciencedirect.com
ScienceDirect
Nuclear Instruments and Methods in Physics Research A 580 (2007) 1066–1070
NUCLEAR INSTRUMENTS & METHODS IN PHYSICS RESEARCH Section A
www.elsevier.com/locate/nima

Position- and time-sensitive single photon detector with delay-line readout

A. Czasch[a,*], J. Milnes[b], N. Hay[b], W. Wicking[b], O. Jagutzki[a,c]

[a]*Institut für Kernphysik, Universität Frankfurt, 60438 Frankfurt, Germany*
[b]*Photek Ltd., St. Leonards on Sea, East Sussex, TN38 9NS, UK*
[c]*RoentDek GmbH, 65779 Kelkheim, Germany*

Available online 30 June 2007

Abstract

We have developed an image intensifier tube with delay-line anode for time- and position-sensitive detection of single photons. By combining two well-approved techniques, the helical-wire delay-line readout for single particle detection and the production capability for large-format sealed photo-multiplier tubes with microchannel-plates, it is possible to build single photon sensors with 40 and 75 mm diameter. Applications are found wherever precise time tagging (<1 ns) in combination with high position resolution (1000×1000 pixel) for single photon detection is of equal importance. Due to the low background this technique is especially suited for imaging at very low light intensity or for "3d" imaging and timing applications such as fluorescence microscopy or coincident photon detection experiments. We present the performance of prototype detectors with 75 mm low-noise S-20 and 40 mm S-20 red-enhanced photo-cathodes.

PACS: 42.79.Pw; 85.60.Gz; 07.57.Kp

Keywords: Photo-multiplier tube; Microchannel-plate; Image intensifier; Delay-line; Photon counting; Time and position detector

1. Introduction

Sealed photo-multiplier tubes (PMTs) with microchannel-plates (MCP) are widely used to intensify faint photon fluxes in the near-UV, visible and near-infrared wavelength regime [1]. A photo-cathode converts photons into electrons. These photo-electrons are multiplied by the microchannel-plate and eventually reconverted to photons by a phosphor screen, preserving the lateral position of the initial photon impact on the photo-cathode. If a so-called image intensifier tube is equipped with double- or triple-stacked MCP operated in saturation, single photons can be counted and imaged. There are similar photo-devices, where the electron charge cloud from the MCP stack is collected on a metal anode and an electrical signal can be picked up. These devices are used to determine the arrival time of single photons with picoseconds' precision; e.g. for time-of-flight measurements (TOF-tube). However, the standard readout technique for image intensifiers (phosphor screen with CCD readout) does not allow for the simultaneous timing of individual photons with sub-nanoseconds' precision, as typically needed for most so-called 3d- imaging applications (timing combined with 2d imaging). Only if the average photon rate is lower than the frame rate of the CCD chip (typically <1000 Hz) it is possible to correlate individual photon positions with a timing signal picked up from the MCP stack.

The alternative method of photo-cathode pulsing for achieving time information on a photon-emitting process can only select a "time window" typically not smaller than about 10 ns width for the photon detection, although the time resolution can be better than this width by using a "fast" phosphor [2]. This method can be very effective under repetitive or triggered experimental conditions. However, since photons outside the time window are not detected, the technically achievable pulse repetition rate (on the order of microseconds) results in a poor duty cycle for randomly arriving photons.

*Corresponding author. Tel.: +49 69 7984 7018; fax: +49 69 7984 7107.
E-mail address: czasch@atom.uni-frankfurt.de (A. Czasch).

0168-9002/$ - see front matter © 2007 Elsevier B.V. All rights reserved.
doi:10.1016/j.nima.2007.06.063

The ideal 3d single photon detector should have a position resolution of at least 1000×1000 pixel, sub-nanosecond time precision and vanishing dead-time between individual photon hits. Sometimes even the detection of photon showers is desirable (multi-hit detection). Furthermore, the average photon detection rate capability should reach the physical limit given by the MCP stack's operation mode of a few MHz. Applications for such a detector are for example found in Neutron radiography [3] and in laser-induced Fluorescence Life-time Imaging Microscopy (FLIM) [4] or spectroscopy (LIF).

There are several approaches to achieve this goal in replacing the phosphor screen by a structured anode. Like in TOF-tubes, the charge cloud from the MCP stack is collected on a metal anode without re-conversion to photons. In the simplest form, a pixel anode can be used with a separate timing electronic channel for each pixel (multi TOF tube).

In order to reduce the number of electronic channels to a practically controllable amount, different anode types with only few specially shaped electrodes or an anode with several corner contacts on a resistive coating can be used [4–10]. Electrical signals from the distinct anode contacts are picked up and their relative pulse heights or time sequence for each photon detection event allow the localization of the charge cloud centre's position, i.e. the position of the photon impact on the photo-cathode. These "position signals" can be easily correlated with a time signal picked up from the MCP stack.

It should be noted that there are also other reasons to apply a pulse counting method for imaging purposes: especially in case of low photon fluxes, the background in the image is much reduced due to the absence of readout noise. Furthermore, there are no saturation effects from long exposure times. This yields better contrast and image dynamics than usually obtainable with phosphor/CCD approaches.

So far none of these attempts could satisfactorily meet all design goals of the "ideal" (3d) single photon detector as defined above. We consider the delay-line technique to be the most promising readout concept because even large-format detectors providing high position resolution can be built. Furthermore, this method potentially allows reaching the limit of high photon fluxes and even multiple photon hits can be analysed.

Delay-line anodes have been used in combination with image intensifier tubes before [8–10]. Approaches with a resistive screen on the tube rear wall and image charge pick-up outside the tube by a "diamond" delay-line array also produced good results and much facilitates the tube construction [11]. However, so far most work focussed on small-format image-intensifier tube of such types with active areas < 40 mm. The helical-wire delay-anode is especially suited for large delay-line arrays (e.g. large detector formats) and can be easily operated in three-layer geometry (Hexanode) with improved efficiency for multiple photon detection events.

In this paper we present tests of a prototype image intensifier tube equipped with an internal helical-wire delay-line anode array. We conclude with an outlook on the perspectives of this detector type.

2. The MCP – PMT with helical-wire delay-line anode

Once the technique of producing sealed MCP–PMTs of large and variable format is established, it is rather straightforward to implement a custom anode behind the MCP stack. But even if most care is taken during the production process, the risks for having a leakage in the ceramics/glass/metal housing assembly will increase with tube size and with the number of electrical feed-through pins. Furthermore, in order to maintain a sufficient vacuum level inside the sealed tube over a long period of several years the anode has to endure extensive cleaning and baking procedures without derogation of the functional anode structures.

Fig. 1 shows a sketch of the PMT with helical-wire delay-line anode (DL-PMT). Two prototypes of different sizes, entrance window materials and photo-cathodes have been built and tested. The DL80-PMT is equipped with a low-noise S-20 photo-cathode of 75 mm diameter on fibre optic window. For the DL40-PMT a red-enhanced S-20 photo-cathode on fused silica window was chosen. The MCP stacks with respective sizes consist of three MCP with 10 μm pores and 60:1 L/D (channel length/diameter ratio).

The helical-wire delay-line anode is placed a few millimetres behind the MCP stack. Due to the choice of material and the robust design the mechanical and electrical properties of the wire array were not affected by the baking and scrubbing processes during production of the tube and the vacuum is well preserved. The helical-wire delay-line array, the readout electronics and the

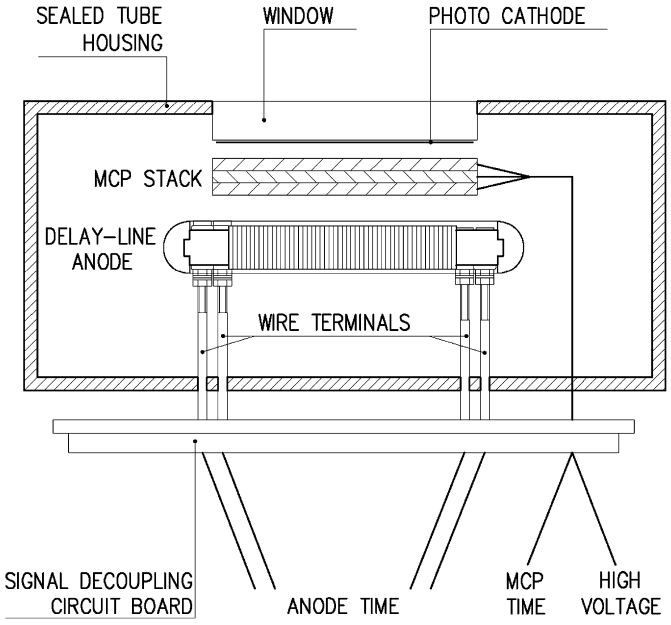

Fig. 1. Sketch of the PMT with helical-wire delay-line anode (DL-PMT).

position encoding method are described extensively in earlier publications [12,13]. In short, wire pairs are wound around a support plate in form of a double-helix. Two perpendicular oriented layers allow for a 2d position determination. The electron charge cloud is collected on the positively biased wire of each pair, almost equally shared between the two layers. The induced electrical signals in the wires (each wire pair forms a differential delay-line) are transmitted to the terminals and are decoupled by capacitors located outside the tube. The four differential signals from the wire array ends are transformed into single-ended 50 Ω impedance signals by adequate circuits. The delay between the signals on both ends of each delay-line is proportional to the position of the charge cloud centre's projection in the respective dimension. The position resolution depends on the time precision for determination of this delay. In order to determine the relative delays with high precision, the signals of about 10 mV mean pulse height and few nanoseconds' width are amplified with low-noise fast amplifiers. Standard CFD (constant fraction discriminator) circuits are used to discriminate electronic noise and to determine the relative signal times with 50 ps precision or better. A fifth, position-independent timing signal can be obtained from the MCP stack: Due to the momentary drain of charge during the electron avalanche emission, a fast voltage drop with positive polarity (1–2 ns width, few 10 mV height) occurs and is picked up via a capacitor from the MCP stack's rear side. This signal is likewise amplified and electronically processed.

The time sequence of these five signals contains the information on the lateral photon absorption point (in the photo-cathode) and on the detection time (neglecting the constant transient time of the electrons and cable delays). The time sequence is registered by time-to-digital converters (TDC) and the position and time information for each photon detection event is computed by a CPU for real-time visualization and event-by-event storage.

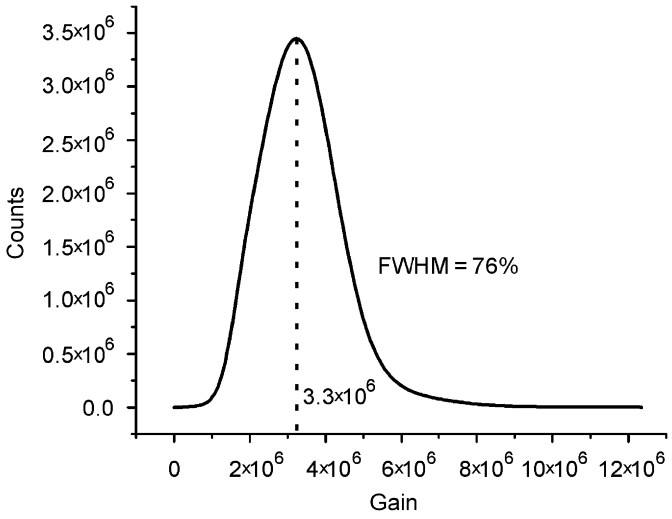

Fig. 2. Pulse-height distribution (gain) of the DL40-PMT's MCP stack at 3000 V.

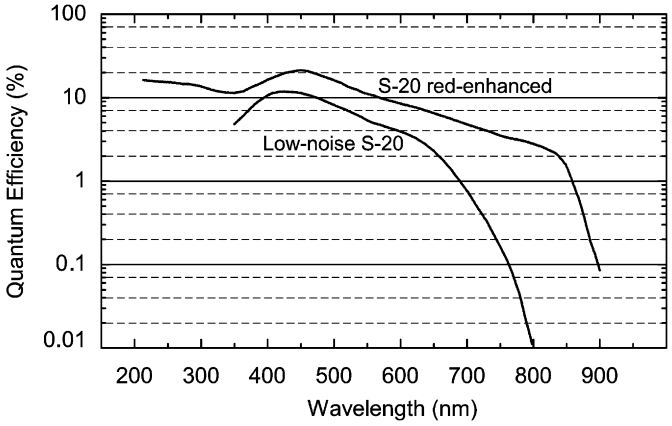

Fig. 3. Photon conversion quantum efficiencies (QE) of the chosen photo-cathodes/window materials as function of the photon wavelength. The decrease at short wavelengths for the DL80-PMT (low-noise S-20) is caused by the vanishing transparency of the fibre optic window for UV-light.

3. Performance of the DL40-PMT and DL80-PMT

The DL40 and DL80 helical-wire delay-line anodes inside the tubes were adopted from standard "open" MCP-delay-line detector systems as used for the detection of charged particles in a vacuum environment. The tests focussed not so much on a detailed detector characterisation but on a feasibility study: Can this technique be extended to sealed photo-tubes maintaining the performance characteristics known from the "open" detectors?

By choosing a triple MCP stack with selected performance parameters, it was possible to achieve the high gain and narrow charge (amount) distribution for single photo-electron detection (Fig. 2) as is required for any single particle detector: every photo-electron's signal is high enough to be discriminated from electronic noise and can be processed after amplification to the timing electronic circuits. Fig. 3 shows the photon conversion quantum efficiencies (QE) of the chosen photo-cathodes as function of the photon wavelength. It should be noted that in spite of the high MCP stack quality only about 75% of the emitted photo-electrons are registered because not all of them give rise to an electron avalanche in the MCP stack. Thus the total detection efficiency is reduced to approximately 75% of the photo-cathode's quantum efficiency.

With the photo-cathode kept at ground potential, a voltage dividing resistor chain provides all necessary voltages for the MCP stack and the wire array from a single high voltage supply. The voltage-dividing and signal decoupling circuits placed just outside the sealed tube are covered by resin for safety. Five coaxial cables deliver the timing signals to the amplifiers and the high voltage is supplied through an adequate shielded cable.

Amplifier/CFD circuits of type *ATR19* and TDCs (*HM1-B* and *TDC8HP*) designed for helical-wire delay-line readout [14] were used during the tests. The images

shown in the following figures are 2d-histograms from a PC-memory. They were accumulated by measuring each photon's signal time sequence, calculating the time difference for both dimensions in the PC RAM and incrementing the corresponding cell of the histogram for every photon counted. The bin size is given by the TDC's channel width of 133 ps (*HM1-B*) or 25 ps (*TDC8HP*). This corresponds to position bins from the delay/mm scaling function of the respective delay-line: about 0.75 ns/mm for the DL40 and 1 ns/mm for the DL80. However, in the following, the "raw" images without position calibration are presented.

Fig. 4 shows images obtained with the DL40-PMT: a shadow mask of 1 mm holes every 3.8 mm was placed in contact with the window and homogenously illuminated (left). The dark emission (thermally emitted electrons) of the red-enhanced S-20 photo-cathode (about 13 000 counts/cm$^2 \cdot$ s at room temperature) is shown on the right. The DL80-PMT's low-noise S-20 photo-cathode produces only < 30 counts/cm^2 s. Both values are within expectations. It is to note that PMTs with standard S-20 or "redder" photo-cathodes should be cooled to about -20 °C in order to reduce the dark count rate to a tolerable level for photon counting. This is a common practise, though it was not

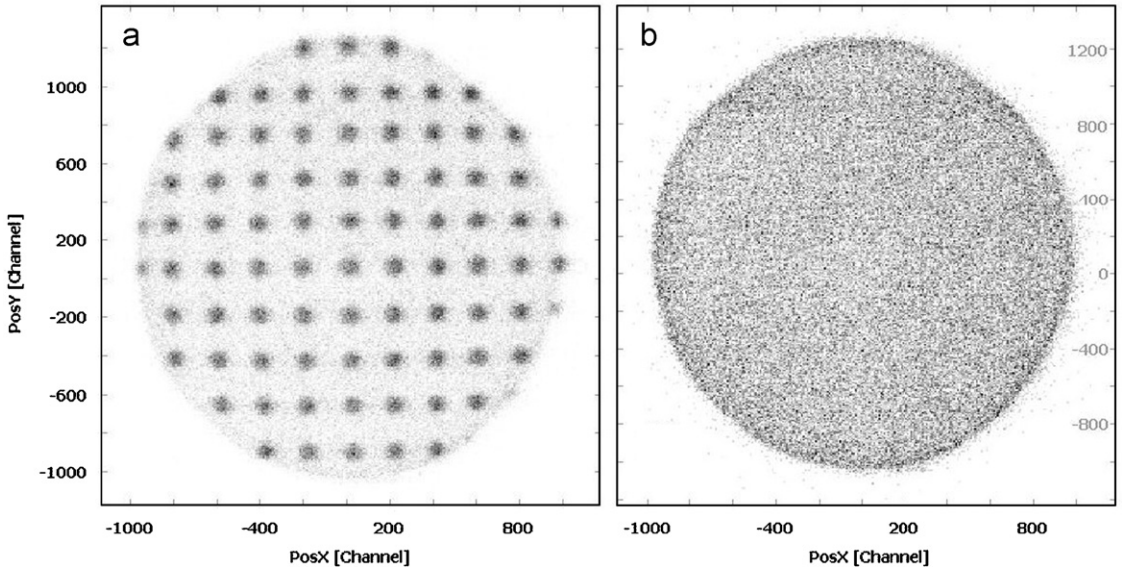

Fig. 4. Images (linear grey scale) of the DL40-PMT: shadow of a homogenously illuminated mask of 1 mm holes every 3.8 mm, placed in contact with the entrance window (a), and noise image (b).

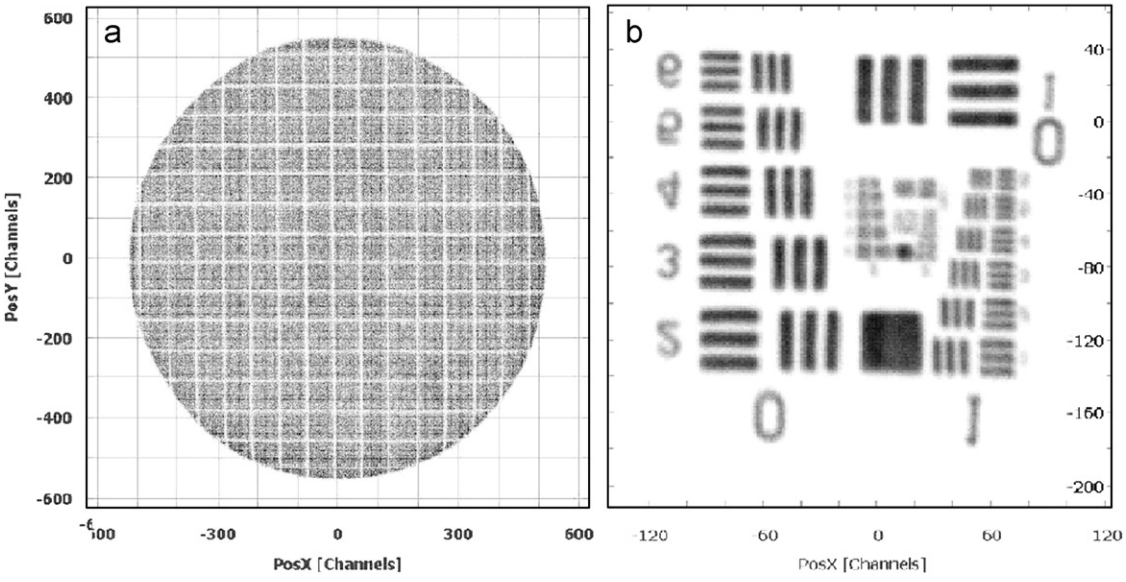

Fig. 5. Image response of the DL80-PMT to shadow masks: grid lines of 1 mm width every 5 mm (a), and NASA test mask (b). The field-of-view in (b) is approximately 20×20 mm, both images in linear gray scale.

applied during the tests presented in this paper. Fig. 5 shows the image response of the DL80-PMT: a shadow masks with 1 mm wide lines every 5 mm (left) demonstrates the homogenous and uniform imaging properties as were expected from tests on similar "open" delay-line detectors. Minor non-linearity can arise from an imperfect wire array and from electrostatic lens effects near the outermost image area. The position resolution of the DL80-PMT in combination with the *HM1-B* TDC could be determined with a standard NASA mask (right) to a FWHM of about 150 μm. This is in accordance with expectations for the effective pixel width of the *HM1-B* (75 μm with DL80). It corresponds to a RMS or pixel resolution of about 1000×1000. By the choice of a "better" TDC (like the *TDC8HP*) the resolution can be further increased. However, this could not yet be demonstrated during the tests on the DL40-PMT with *TDC8HP* due to the high thermal background (the *TDC8HP* was not yet available during tests of the DL80-PMT). It is expected from results on open delay-line detectors that 1000×1000 pixel resolution for the DL40-PMT and 2000×2000 pixels for the DL80-PMT is achieved in combination with the *TDC8HP* or similar highly resolving TDCs with LSB < 50 ps.

The photo-electron rates during all these tests where kept between 1000 and 1 million counts/s because higher count rates could not be registered by the TDCs. No saturation effects or image degradation are observed in this regime. Tests on the absolute time resolution could not be done due to the lack of a pulsed photon source. However, since the position is determined through timing signals, one can expect that the good imaging characteristic coincides with an equally well timing response.

4. Summary and outlook

In summary, the results of these tests confirm that all performance characteristics of open delay-line detectors are reproduced in DL-PMT-type photon detectors and that known properties from standard image intensifier tubes (photo-cathode response, gain) are also preserved for a DL-PMT. It is thus possible to design DL-PMT tubes for a specific application (photo-cathode type, effective detection diameter, etc.) and scale the typical performance parameters from experiences on existing detectors.

It should be straightforward to increase the effective image diameter to at least 120 mm and to implement a Hexanode delay-line type for multi-hit applications [15]. Next-generation TDC circuits will allow a detection rate increase to over 1 megacounts/s. Thus it can be expected that the "ideal" time and position-sensitive single photon detector can soon be realized using DL-PMT-type image intensifiers.

Due to the superior imaging properties of pulse counting methods it would be desirable to also use such detectors for pure imaging applications. This seems feasible for photon rates up to 10 megacounts/s. Beyond this rate physical limits of MCP recovery and delay-line response dead-time are difficult to overcome. Therefore this technique cannot replace completely fast ICCD cameras with high frame rates and/or pulsed photo-cathodes.

References

[1] 〈http://www.photek.comorothermanufacturershomepages〉.
[2] V. Dangendorf, A. Breskin, R. Chechik, G. Feldman, M.B. Goldberg, O. Jagutzki, C. Kersten, G. Laczko, I. Mor, U. Spillmann, D. Vartsky, Nucl. Instr and Meth. A 535 (2004) 93.
[3] V. Dangendorf, G. Laczko, C. Kersten, O. Jagutzki, U. Spillmann, In: P. Chirco, R. Rosa (Eds.), Proceedings of the Seventh World Conference, Vol. 7, Rome, Italy, September 15–21, 2002, ENEA, Public Relations Department-Communication Unit, Rome, 2005, p. 383 〈http://www.arxiv.org/abs/nucl-ex/0301001〉.
[4] V. Emiliani, D. Sanvitto, M. Tramier, T. Piolot, Z. Petrasek, K. Kemnitz, C. Durieux, M. Coppey-Moisan, Appl. Phys. Lett. 83 (2003) 2471.
[5] L.A. Kelly, J.G. Trunk, J.C. Sutherland, Rev. Sci. Instrum. 68 (1997) 2279.
[6] J.R. Powell, J.R. Howorth, M.B. Ingle, Proc. SPIE 2198 (1994) 400.
[7] J.S. Lapington, L.B. Boskma, J. Adema, Proc. SPIE 2198 (1994) 851.
[8] S.E. Sobottka, M.B. Williams, IEEE Trans. Nucl. Science NS-35 (1988) 348.
[9] C. Ho, K.L. Albright, A.W. Bird, J. Bradley, D.E. Casperson, M. Hindman, W.C. Priedhorsky, W.R. Scarlett, R. Clayton Smith, J. Theiler, S. Kerry Wilson, Appl. Opt. 38 (1999) 1833.
[10] X. Michalet, O.H.W. Siegmund, J.V. Vallerga, P. Jelinsky, J.E. Millaud, S. Weiss, Proc. SPIE 6092 (2006) 60920M.
[11] O. Jagutzki, J.S. Lapington, L.B.C. Worth, U. Spillmann, V. Mergel, H. Schmidt-Böcking, Nucl. Instr. and Meth. A 477 (2002) 256.
[12] O. Jagutzki, V. Mergel, K. Ullmann-Pfleger, L. Spielberger, U. Spillmann, R. Dörner, H. Schmidt-Böcking, Nucl. Instr. and Meth. A 477 (2002) 244.
[13] O. Jagutzki, V. Mergel, K. Ullmann-Pfleger, L. Spielberger, U. Meyer, R. Dörner, H. Schmidt-Böcking, Proc. SPIE 3438 (1998) 322.
[14] 〈http://www.roentdek.com〉.
[15] O. Jagutzki, A. Czasch, R. Dörner, M. Hattaß, V. Mergel, U. Spillmann, K. Ullmann-Pfleger, T. Weber, H. Schmidt-Böcking, A. Cerezo, M. Huang, G. Smith, IEEE Trans. Nucl. Sci NS-49 (2002) 2477.